

Effect of pressure on the electric-field-induced resistance switching of VO₂ planar-type junctions

Joe Sakai*

Laboratoire LEMA, UMR 6157 CNRS-CEA, Université François Rabelais, Parc de Grandmont, 37200 Tours, France

Makio Kurisu

School of Materials Science, Japan Advanced Institute of Science and Technology, 1-1 Asahidai, Nomi, Ishikawa 923-1292, Japan

(Received 9 January 2008; revised manuscript received 9 April 2008; published 11 July 2008)

VO₂ thin-film planar-type junctions with the size of 1500 μm in width and 10 μm in length were fabricated on Al₂O₃ (0001) substrates, and the electric-field-induced resistance switching (EIRS) characteristics were investigated at hydrostatic pressures up to 2 GPa and room temperature. The resistance in the electric-field-induced low resistance state (E-LRS) was revealed to be insensitive to the hydrostatic pressure, in contrast to the apparent suppression of resistance in the temperature-induced low resistance state. The critical current to induce E-LRS is increased as the pressure is increased, while the voltage at the transition is independent of the pressure. These results indicate a picture in VO₂ that not a Joule heating but a reversible breakdown triggers EIRS, and that the electric current of huge density maintains filamentary E-LRS regions.

DOI: 10.1103/PhysRevB.78.033106

PACS number(s): 71.30.+h, 62.50.-p, 77.22.Jp

It has been known for half a century that vanadium dioxide VO₂ shows a structural phase transition at about 340 K from monoclinic MoO₂ type to tetragonal rutile type structure, accompanied by a sharp insulator-metal (IM) transition with a several-order change in its resistivity, sometimes called as the “temperature-induced resistance switching (TIRS).”¹ On the other hand, an electric-field-induced IM transition of VO₂ has also been reported several decades ago.² The current-voltage (*I-V*) characteristics of a VO₂ bulk sample possess a gradual change of the resistance,^{3,4} while that of a VO₂ thin-film sample shows an extremely steep and discontinuous jump of resistance at the transition.⁵⁻⁷ We note here that these *I-V* characteristics are symmetric about the origin, and therefore, this is a phenomenon different from that found in so-called resistance random access memory. Since anomalous novel physical properties have been revealed in a variety of strongly correlated electronic oxide materials, the electric-field-induced resistance switching (EIRS) of VO₂ is attracting much attention again, and researches aiming at new applications of VO₂ are progressing.⁸⁻¹¹

A similar EIRS has been found in Pr_{1-x}Ca_xMnO₃ (PCMO). PCMO with a certain Ca content *x* (0.3 ≤ *x* ≤ 0.75) realizes a charge ordered (CO) state, in which trivalent and tetravalent Mn ions are ordered alternately in the *ab* plane.¹² Application of an electric field exceeding a threshold value to a PCMO material in the CO state causes a resistance switching.¹³⁻¹⁵ This IM transition is considered to originate in a collapse of the CO state caused by the electric field. The charge ordering temperature is relatively lower in PCMO, 240 K.¹² On the other hand, VO₂ is promising in the application for switching devices and so on, since it shows EIRS at room temperature.

However, the mechanism of EIRS in VO₂ has not been fully established. All the vanadium ions are tetravalent in the case of VO₂, therefore a CO state is not expected to occur in it. It has been clarified by several optical microscope observations that the electric-field-induced low resistance state (E-LRS) appears as a localized filamentary conductive path.¹⁶⁻¹⁸ Since the first report of EIRS,² many researchers have as-

sumed that it is the Joule heat that triggers EIRS, and also maintains the filamentary conductive paths in VO₂.¹⁹ Thus far, however, no direct temperature measurement has been done for a conductive VO₂ filament of 10⁰–10¹ μm in width. On the other hand, Kim *et al.*⁸ have performed a micro-Raman observation on a VO₂ planar-type junction that undergoes EIRS and reported the occurrence of an insulator-metal transition prior to a structural phase transition. This result suggests a possibility that something other than the Joule heat triggers EIRS.

In order to reveal what triggers EIRS and what maintains E-LRS, it should be effective to introduce another external parameter to tune the phenomena. Here, we chose the pressure as an external thermodynamic parameter and examined its influences on EIRS in a VO₂ thin film. Previously, the pressure dependence of the resistance in the high resistance state (HRS), *R_H*, and the resistance in the temperature-induced low resistance state (T-LRS), *R_{T-L}*, have been investigated.²⁰⁻²² However, there has been no report on the pressure dependence of the resistance in E-LRS, *R_{E-L}*, and the transition voltage, *V_{tr}*, of VO₂. In the present study, we investigated the *I-V* characteristics of VO₂ planar-type junctions at hydrostatic pressures up to 2 GPa to reveal the mechanism of EIRS. Comparison of the pressure dependences of *R_{E-L}* and *R_{T-L}*, as well as optical microscope observations, suggest the factor to maintain E-LRS, whereas the pressure dependences of transition parameters imply what triggers EIRS.

VO₂ thin films were fabricated by a pulsed laser deposition technique. A focused KrF excimer laser beam was shot on a metallic vanadium target with the fluence of 3 J/cm² at a repetition rate of 10 Hz, in O₂ gas of 20 mTorr. The films were deposited on Al₂O₃ (0001) single-crystal substrates maintained at 500 °C for 30 min, resulting in the film thickness of 220 nm. Figures 1(a) and 1(b) show respectively an x-ray diffraction (XRD) profile at room temperature and the temperature dependence of the resistivity (*ρ-T*) of a VO₂ thin film thus prepared. The XRD pattern shows only a (020) reflection peak from the VO₂ thin film, indicating that the film is single-oriented with no second phase. The *ρ-T* curve

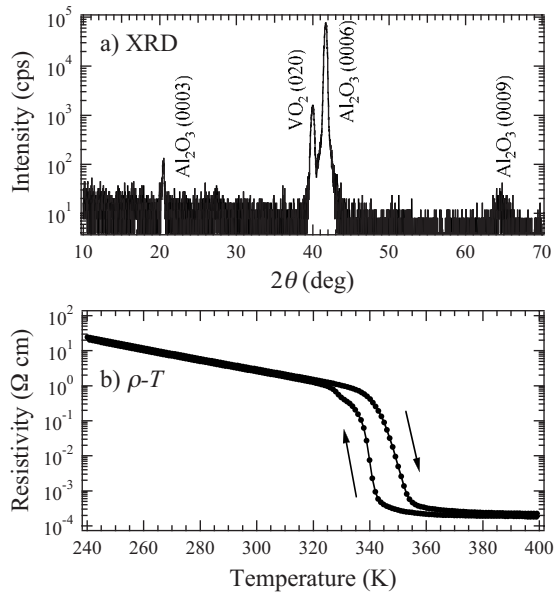


FIG. 1. (a) An XRD profile and (b) the temperature dependence of the resistivity, of a VO_2 thin-film deposited on an Al_2O_3 (0001) substrate.

shows TIRS at 340–350 K where a four-order drop of the resistivity is observed. This TIRS, as well as a composition analysis by a Rutherford backscattering measurement (not shown), confirms that this film consists of stoichiometric vanadium dioxide.

The planar-type junctions were fabricated by the following process; the VO_2 film on the Al_2O_3 substrate was patterned using conventional photolithography and electron cyclotron resonance etching techniques, and then an Au/Ti bilayered film for electrodes were deposited on the VO_2 film and patterned by a lift-off method. A $5 \times 5 \text{ mm}^2$ substrate with nine junctions was cut into three $1.5 \times 2.6 \text{ mm}^2$ chips. One chip containing three junctions each of which having the size of $10 \mu\text{m}$ in length (=gap between electrodes) and $1500 \mu\text{m}$ in width was then fixed on a stage for the resistive measurements. The voltage and current leads (Au) were ultrasonically bonded to electrode pads on the junctions, and the other ends of the leads were soldered to electrode pins of the stage. Hydrostatic pressure was generated using a clamp-type piston-cylinder device with the pressure-transmitting medium of 1:1 mixture of *n*-pentane and isoamyl alcohol. A manganin manometer was used to determine the pressure value at room temperature.

The I - V characteristics of the junctions were measured by means of a two probe method using a personal computer controlled current source and monitor instrument (ADC Co., R6243) at room temperature and pressures up to 2 GPa. Here we swept the current at a constant rate and measured the junction voltage. It took 5 s to complete one cyclic I - V measurement. No load resistor was inserted in the I - V measurements circuit in series to the VO_2 planar-type junction because we had found that the existence of a series resistance component affects greatly the I - V behavior of the sample in which EIRS is observed.²³

Figure 2 shows the I - V characteristics of a VO_2 planar-

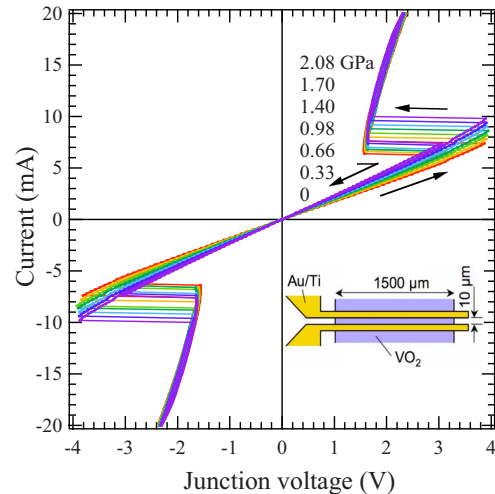


FIG. 2. (Color online) I - V characteristics of a VO_2 planar-type junction under various hydrostatic pressures. Inset shows a schematic drawing of the junction.

type junction under various hydrostatic pressures. An extremely sharp resistance switching was observed, appearing as an infinite negative-differential-resistance region. The existence of a hysteresis suggests that this transition is a first-ordered one. As reported previously,⁵ the electrical properties are independent of the current direction, implying that the nonlinear property is not caused by a Schottky barrier. One may notice that the asymptotic line of the I - V trace in the E-LRS region does not pass the origin but crosses the voltage axis at approximately 1 V, probably because of a flexibility of the filament width as discussed below. For this reason, a differential resistance ($=dV/dI$) is considered to be more appropriate to describe the resistive behavior of the junction at E-LRS, rather than a static resistance ($=V/I$). In what follows we define R_{E-L} as the inversed gradient between two points corresponding to $I=19$ and 20 mA , and R_H as the static resistance near the origin.

The resistance in HRS clearly decreases as the pressure increases, while the behavior in E-LRS appears to be less sensitive to the pressure. Pressure dependences of R_H and R_{E-L} are shown in Figs. 3(a) and 3(b), respectively. Following Ladd *et al.*,²¹ we attempted to describe the pressure dependence of R_H and R_{E-L} by $d \ln R/dp = a$, where a is the attenuation constant and p is the pressure. The least-square fitting was made, giving the attenuation constant $a = -0.127 \text{ GPa}^{-1}$ for R_H . This suppression behavior of R_H by the external pressure is quite similar to a VO_2 bulk single crystal case where $a = -0.15 \text{ GPa}^{-1}$.²¹ On the other hand, R_{E-L} was found to be hardly affected by the hydrostatic pressure, with a small attenuation constant $a = -0.025 \text{ GPa}^{-1}$. This value is considerably smaller than that previously reported for a bulk VO_2 in the T-LRS where a is in the order of 10^{-1} GPa^{-1} .^{20,22} This implies that E-LRS is totally different from T-LRS in the pressure response.

Then a question arose, whether the crystal structure of VO_2 in E-LRS is the same as that in T-LRS or not. In order to obtain information about it, we performed optical microscope observations to compare the colors of one VO_2 junction in E-LRS and in T-LRS. As the result, the junction

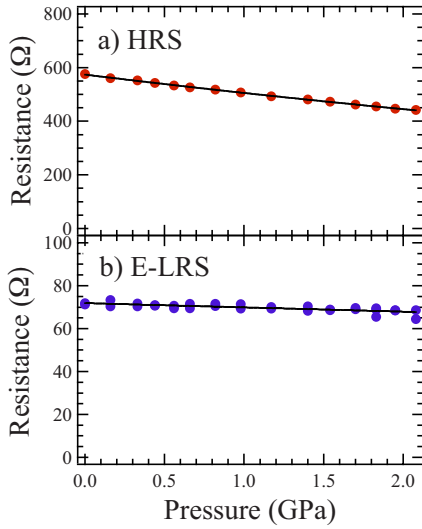


FIG. 3. (Color online) The hydrostatic pressure dependences of (a) the static resistance near the origin in HRS ($=R_H$), and (b) the differential resistance in E-LRS ($=R_{E-L}$). The solid lines are fitting curves for exponential pressure dependence of R_H and R_{E-L} .

showed an identical color in both states (Fig. 4). Therefore we conclude that the crystal structure of VO_2 in E-LRS is most likely tetragonal, the same as in T-LRS. Figure 4 also shows a change of the filament width according to the current, similarly to the previous reports.^{16,17} This phenomenon implies a peculiar feature that the current density in the filamentary conductive path tends to be constant. Moreover, the current density is estimated to be as huge as 10^6 A/cm², assuming the resistivity of the nonfilamentary regions to be that in the monoclinic phase at room temperature and using the values of filament width (Fig. 4), film thickness, and current. These observations strongly indicate that E-LRS of filamentary nature is a phase that is controlled and maintained by an electric current.

As for the reason for different pressure dependence between R_{E-L} and R_{T-L} in spite of the same crystal structure of

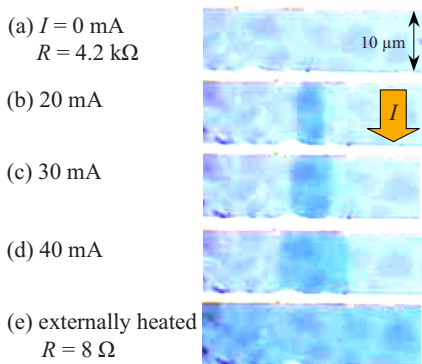


FIG. 4. (Color online) Optical microscope images of a VO_2 planar-type junction with a junction current of (a) 0, (b) 20, (c) 30, and (d) 40 mA at room temperature, and (e) no current fed but heated by an external heater. Dark-color areas correspond to LRS regions. Junction resistance values are noted in (a) and (e), indicating that T-LRS is realized in (e). Contrast of the colors is emphasized equally in all panels.

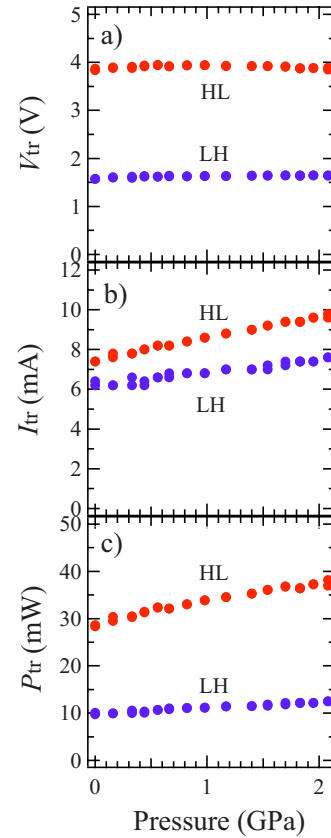


FIG. 5. (Color online) The hydrostatic pressure dependences of (a) the critical voltage V_{tr} , (b) the current I_{tr} , and (c) the power P_{tr} at the EIRS transition points from HRS to E-LRS (labeled as HL) and from E-LRS to HRS (LH).

E- and T-LRS, we consider two candidates. First, the temperature of the E-LRS filamentary path could be different from 74 °C at which the R_{T-L-p} measurement was performed in Ref. 20. Even after the assignment of the crystal structure, we still question whether the temperature at the filamentary E-LRS region reaches 340 K. To clarify it, one needs a temperature measurement of the local region in the filament, which we consider as a future subject. Second, a huge current density as 10^6 A/cm² in the filamentary path of E-LRS brought about a pressure response different from that of T-LRS, which was probably investigated with a small current in Ref. 20. Large current density would possibly cause a strong correlation of electrons and a deviation from a band theory. Hence the interpretation of R_{T-L-p} given in Ref. 20 using a small-band-overlap model may not be applicable to R_{E-L-p} . Either candidate would lead us to have a picture that a current of huge density maintains the tetragonal structure of VO_2 by keeping the channel open, instead of a picture that a current causes a temperature-induced structural phase transition through a Joule heating.

Now we focus on the critical parameters at the transition in order to discuss the triggering mechanism of EIRS in the VO_2 film. Figures 5(a)–5(c) show the pressure dependences of the critical voltage V_{tr} , the current I_{tr} , and the power P_{tr} , respectively, at the transition points from HRS to E-LRS and vice versa. V_{tr} was found to be independent of the pressure. V_{tr} of 4 V and the junction length of 10 μm give the transi-

tion electric field E_{tr} of 4×10^3 V/cm. On the other hand, I_{tr} obviously increases as the pressure increases. This is related to the behaviors of R_H that decreased and V_{tr} that did not change. Consequently P_{tr} , the product of V_{tr} and I_{tr} , increases with the pressure.

Assuming if the observed EIRS in the present VO₂ sample is triggered by a Joule heat, T_{tr} should obey the Fourier's law for heat conduction in solid

$$T_{tr}(p) - T_R = \frac{P_{tr}(p)t}{c(p)m}, \quad (1)$$

where T_R is the room temperature, t the time for power input, c the specific heat of VO₂, and m the mass of the VO₂ channel in which the transition occurs. The increase in T_{tr} was previously reported to be by no more than 1.2–1.6 K at a pressure of 2 GPa.^{20,21} This means that $[T_{tr}(p) - T_R]$ increases only by 3%–4%. On the other hand, the present experimental results show that P_{tr} increases by $\sim 40\%$ under a pressure of 2 GPa [Fig. 5(c)]. Supposing that Eq. (1) is still satisfied after a 4% increase of $[T_{tr}(p) - T_R]$ and a 40% increase of $P_{tr}(p)$, we should examine a possibility that the specific heat c increased by 35% by the pressure of 2 GPa. In general, however, as the Debye temperature is an increasing function of pressure, the specific heat should decrease as the pressure increases. Thus it seems to be less realistic that a Joule heat triggers EIRS.

It is noteworthy that I_{tr} is pressure dependent while V_{tr} is not [Figs. 5(a) and 5(b)], indicating that the electric field plays more important role than the current does to trigger EIRS. This allows us to assume a model that EIRS is a type of reversible electrical breakdown. Generally, it is known that an avalanche breakdown occurs in insulators when the applied electric field becomes high enough to accelerate free electrons up to a velocity that enables them to excite additional electrons. It appears plausible to consider EIRS in VO₂

to be an avalanche breakdown phenomenon by assuming that the dielectric strength of the present junction is 4×10^3 V/cm, two orders smaller than that of conventional semiconductor materials. In other words, E-LRS of VO₂ is possibly triggered by an electrical breakdown and is maintained by a current of huge density, instead of being triggered and maintained by a Joule heat as has been believed. A previous study of EIRS containing multisteps during the transition from HRS to E-LRS also support the model of the electrical breakdown.⁵ So smaller $P(=IV)$ after the transition than before the transition may prevent from any thermal degradation such as disorder of the atomic structure or change of the composition, and thus may make this electrical breakdown reversible. From the present results, we also note that materials with low dielectric strength such as 10^3 V/cm or less would possibly be candidates to achieve EIRS that would be applied for novel switching devices.

In conclusion, we observed EIRS of VO₂ thin-film planar-type junctions at hydrostatic pressures up to 2 GPa and room temperature, and investigated the pressure dependences of various properties characteristic to EIRS. The differential resistance of the junction in E-LRS is insensitive to the pressure, in contrast to the resistance of a VO₂ in T-LRS, supporting a picture that a current flow of a huge density maintains the E-LRS region. The input power at EIRS transition increased by 40% under a pressure of 2 GPa, implying that the observed EIRS is triggered by different mechanism from TIRS. The result that the transition voltage is pressure independent indicates that the direct trigger of EIRS is the electric field, and that EIRS can be described as an avalanche breakdown in VO₂ with a dielectric strength much lower than that of conventional semiconductors.

The authors are grateful to K. Okimura at Tokai University for the helpful discussions. This work was partially supported by the Kazuchika Okura Memorial Foundation.

*jo.sakai@univ-tours.fr

¹F. J. Morin, Phys. Rev. Lett. **3**, 34 (1959).

²P. F. Bongers and U. Enz, Philips Res. Rep. **21**, 387 (1966).

³Y. Taketa, F. Kato, M. Nitta, and M. Haradome, Appl. Phys. Lett. **27**, 212 (1975).

⁴B. Fisher, J. Appl. Phys. **49**, 5339 (1978).

⁵K. van Steensel, F. van de Burg, and C. Kooy, Philips Res. Rep. **22**, 170 (1967).

⁶C. N. Berglund and R. H. Walden, IEEE Trans. Electron Devices **17**, 137 (1970).

⁷J. C. Duchene, M. M. Terrailon, M. Pailly, and G. B. Adam, IEEE Trans. Electron Devices **18**, 1151 (1971).

⁸H. T. Kim, B. G. Chae, D. H. Youn, G. Kim, K. Y. Kang, S. J. Lee, K. Kim, and Y. S. Lim, Appl. Phys. Lett. **86**, 242101 (2005).

⁹K. Okimura, Y. Sasakawa, and Y. Nihei, Jpn. J. Appl. Phys., Part 1 **45**, 9200 (2006).

¹⁰F. Dumas-Bouchiat, C. Champeaux, A. Catherinot, A. Cruntéanu, and P. Blondy, Appl. Phys. Lett. **91**, 223505 (2007).

¹¹J. Sakai, J. Appl. Phys. **103**, 103708 (2008).

¹²Z. Jirak, S. Krupicka, Z. Simsa, M. Dlouha, and S. Vratilav, J. Magn. Magn. Mater. **53**, 153 (1985).

¹³A. Asamitsu, Y. Tomioka, H. Kuwahara, and Y. Tokura, Nature (London) **388**, 50 (1997).

¹⁴J. Sakai, A. Kitagawa, and S. Imai, J. Appl. Phys. **90**, 1410 (2001).

¹⁵T. Murakami, J. Sakai, and S. Imai, J. Appl. Phys. **94**, 6549 (2003).

¹⁶J. Duchene, M. Terrailon, P. Pailly, and G. Adam, Appl. Phys. Lett. **19**, 115 (1971).

¹⁷C. N. Berglund, IEEE Trans. Electron Devices **16**, 432 (1969).

¹⁸B. Fisher, J. Phys. C **8**, 2072 (1975).

¹⁹A. Mansingh and R. Singh, J. Phys. C **13**, 5725 (1980), and references therein.

²⁰C. N. Berglund and A. Jayaraman, Phys. Rev. **185**, 1034 (1969).

²¹L. A. Ladd and W. Paul, Solid State Commun. **7**, 425 (1969).

²²C. H. Neuman, A. W. Lawson, and R. F. Brown, J. Chem. Phys. **41**, 1591 (1964).

²³T. Murakami, J. Sakai, and S. Imai, Phys. Rev. B **75**, 064423 (2007).